

***Ab Initio* Study of the Electronic and Optical Properties of Hexagonal and Cubic $Ge_2Sb_2Te_5$**

Henry Odhiambo^{1,*}, George Amolo², Nicholas Makau², Felix Dusabirane²,
Herick Othieno¹ and Andrew Oduor¹

¹Maseno University, Department of Physics and Materials Science, Maseno, Kenya

²University of Eldoret, Department of Physics, Computational Materials Science Group,
Eldoret, Kenya

The electronic and optical properties of hexagonal and cubic $Ge_2Sb_2Te_5$ have been calculated using the QUANTUM ESPRESSO and Yambo codes. The study has considered the variation of electronic band gaps with lattice constants using the LDA with non-linear correction, where it was established that both phases are apparently metallic at equilibrium. Upon increasing a , it was found that the hexagonal phase had a maximum gap of 0.22 eV at a c/a value of 3.49 whereas the cubic phase had a maximum gap of 0.23 eV at a much higher c/a value of 10.62. Findings of the optical absorption spectra of both hexagonal and cubic $Ge_2Sb_2Te_5$ obtained using time dependent density functional theory (TDDFT) and the partially self-consistent GW (GW_0) are also reported. The absorption edge has been observed at 0.48 eV using TDDFT and at 0.21 eV using GW_0 for the hexagonal phase.

1. Introduction

Phase change materials such as ternary alloys along the pseudobinary line $(GeTe)_x(Sb_2Te_3)_y$ are often used in optical storage media such as rewritable compact disks (CD-RW), digital versatile disks (DVDs), and blu-ray disks (BDs). Recently, phase change materials have been considered as natural candidates for electronic memory applications [1,2]. Phase change memory relies on a rapid and reversible, thermally induced amorphous phase to crys-talline phase transition [1,3]. The transition is accompanied by a change in reflectance (depending on layer thickness and wavelength) of up to 30% [4], as well as a change in the resistivity of several orders of magnitude [2]. In spite of the great technological significance of phase change materials, some of their fundamental properties such as optical absorption are yet to be clearly understood [4].

Among phase change materials, $Ge_2Sb_2Te_5$ (GST) is the most studied and widely applied due to its superior performance in terms of speed of transformation (~ 50 ns) and stability in the amorphous phase [5]. GST has two crystalline phases; a metastable cubic phase, which undergoes the reversible crystalline to amorphous transition, and a stable hexagonal phase [6-8].

The hexagonal phase has $P3m1$ symmetry and nine atoms per unit cell in nine layers stacked along the c -axis. Petrov et al. [7] proposed the sequence $Te-Sb-Te-Ge-Te-Te-Ge-Te-Sb$. Kooi and de Hosson [8] proposed the sequence $Te-Ge-Te-Sb-Te-Te-Sb-Te-Ge$ in which the positions of Ge and Sb are interchanged. Recently, Matsunaga et al. [6] have proposed a disordered phase in which Sb and Ge atoms randomly occupy the same layer resulting in a mixed configuration. In this study, the sequence of Kooi and de Hosson (Fig. 1), which apparently has the lowest total energy [9], has been considered. The cubic phase has a rock salt-like structure in which Te atoms occupy the anion ($4a$) sites whereas Ge atoms, Sb atoms and intrinsic vacancies occupy randomly the cation ($4b$) sites [5,10-13]. In this study, cubic GST has been replaced by an equivalent hexagonal lattice by taking layer ordering along the [111] direction in the rock salt-like structure. This results in a unit cell having 27 atoms and three vacancies (v) arranged along the c -axis in the stacking sequence $Te-Ge-Te-Sb-Te-v-Te-Sb-Te-Ge$ repeated three times (Fig. 2) [14].

This work considers the treatment of Te 4d electrons either as core or semicore and with different exchange-correlation (XC) terms, in this case, the local density approximation (LDA) and the generalized gradient approximation (GGA). We further explore electronic band gap dependence on lattice parameters within the LDA for the XC term. Using the LDA, Tsafack et al. [15] stopped short of

* henod2001@yahoo.com

estimating the optical band gap using the intersection of $(\alpha\hbar\omega)^{1/2}$ with the energy axis, $\hbar\omega$. This was due to a discrepancy in the calculated absorption coefficient, $\alpha(\omega)$. As an extension to the static DFT analysis of Tsafack et al. [15], this work attempts to estimate the optical band gaps of hexagonal and cubic GST from their optical absorption spectra, calculated using time dependent density functional theory (TDDFT) and the partially self consistent GW (GW_0).

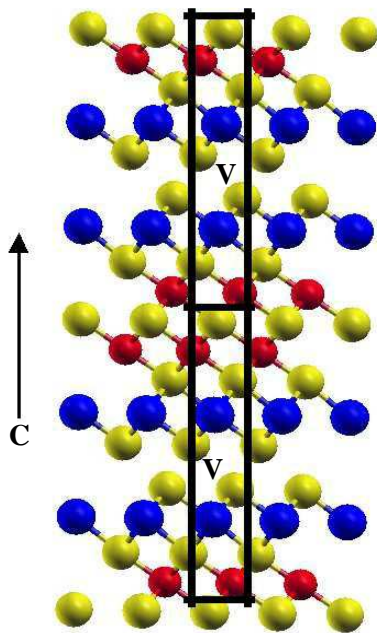


Fig.1: Hexagonal GST structure showing *Te* (yellow), *Ge* (red) and *Sb* (blue) atoms and intrinsic vacancy layers, *v*. Solid lines indicate the unit cell.

2. Computational Details

The electronic structure calculations reported in this study were performed within the framework of DFT [16,17] as implemented in the QUANTUM ESPRESSO code [18] which expands the Kohn-Sham orbitals on a plane wave basis set. The LDA Perdew and Zunger (PZ) [19] and the GGA Perdew-Becke-Ernzerhof (PBE) [20] have been considered for the XC energy functional. The interactions between atomic cores and electrons were described using non-relativistic norm-conserving pseudopotentials with non-linear correction and with semicore electrons. Subsequently, the valence configurations in both cases is *Ge* $4s^24p^2$, *Sb* $5s^25p^3$, *Te* $5s^25p^4$ with *Ge* $3d$, *Sb* $4d$ and *Te* $4d$ electrons being treated as semicore

in the latter case. Lee and Jhi [21] and Do et al. [22] have shown that including the *Te* $4d$ electrons in the valence configuration has an effect on the value of the calculated lattice constants. Van Lenthe *et al* [23] have noted the effect of spin-orbit coupling on bond distances (and hence lattice constants) in such heavy atoms as *Te*, *Sb* and *Ge*. An accurate description of spin-orbit coupling requires a relativistic treatment. However, as already noted, relativistic effects were not taken into account in constructing the pseudopotentials used in this study.

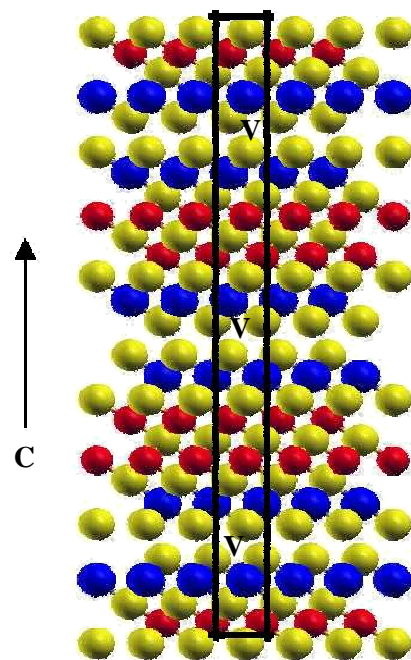


Fig.2: Cubic GST structure showing *Te* (yellow), *Ge* (red) and *Sb* (blue) atoms and intrinsic vacancy layers, *v*. Solid lines indicate the unit cell.

Brillouin zone (BZ) integration was performed using an unshifted k-point grid of $8 \times 8 \times 2$, generated according to the Monkhorst-Pack (MP) scheme [24], with a cut-off energy of 50 Ry for both GST phases.

The lattice parameters were optimized by fitting the energy versus volume data to the Murnaghan Equation of State (EOS) [25]. The atomic positions were subsequently optimized at the equilibrium lattice parameters. The electronic band structures were calculated at the equilibrium lattice parameters. In addition, the dependence of the electronic band gap energy on lattice parameters has been investigated.

Processes that involve electronic excitation are many-body in nature and are accessible via many-body perturbation theory (MBPT) and TDDFT amongst others. In this study, the optical absorption spectra of hexagonal and cubic GST structures were calculated using TDDFT, implemented within turboTDDFT [26], and the partially self-consistent GW (GW_0) as implemented in the Yambo code [27].

3. Results

3.1. Electronic properties

The electronic band structures and the corresponding density of states for hexagonal and cubic GST were computed at the equilibrium lattice parameters as already stated. The LDA and the GGA were considered for the XC energy functional with the *Te 4d* orbitals being treated as core in the former case and as semicore in the latter case. The inclusion or omission of the *Te 4d* orbitals in the valence states has an influence on the calculated lattice constants [22,28,29], which in turn affect the energy gap values. The LDA calculations apparently show that no band gap exists for both hexagonal (Fig. 3) and cubic GST (Fig. 5). In particular, the top of the valence band and the bottom of the conduction band are degenerate at Γ , suggesting that hexagonal GST is apparently semi-metallic whereas for cubic GST, the Fermi level is located slightly inside the valence band indicating that it possesses metallic character. The GGA calculations show for the hexagonal phase a band gap of about 0.33 eV at Γ (Fig. 4) and for the cubic phase a band gap of about 0.24 eV at Γ and an indirect band gap of about 0.04 eV along the Γ -K line (Fig. 6).

In general, the GGA and LDA results give band gaps that are less than the experimental optical band gap of 0.5 eV for both phases [30,31]. In comparison, Lee and Jhi [21] have calculated an indirect band gap of 0.26 eV along the Γ -K line for the sequence proposed by Kooi and de Hosson [8]. Tsafack et al. [15] have reported a semi-metallic behavior for the sequence of Kooi and de Hosson [8] and an indirect band gap of about 0.2 eV along the Γ -K line for the cubic phase. Differences in the calculated band gap values between the theoretical studies mentioned above and this work lies in the approximation for the XC energy functional and treatment of the *Te 4d* electrons. The use of different XC-terms, and the treatment of *Te 4d* electrons as core or semicore, results in different lattice parameters and hence band gap values [15]. Moreover, the underestimation of the band gap is a

well-known limitation of DFT since it does not take into account many-body effects; DFT [16,17] fails to give reliable quantitative values for the band gaps of insulators and semiconductors, which are often underestimated by as much as 1.0 eV or more [32]. Strong electronic correlation and exchange can be included using hybrid functionals, projector augmented wave (PAW) methods, quantum monte carlo (QMC) methods, MBPT and TDDFT among others. Using the projector augmented wave (PAW) method with GGA, Park *et al* [33] have calculated band gap values of 0.41 eV and 0.51 eV for hexagonal and cubic GST, respectively.

Due to the fact that different XC terms and the treatment of *Te 4d* states could result in different lattice parameters, the dependence of electronic band gap on lattice parameters for hexagonal and cubic GST was calculated using the LDA for the XC energy functional and the findings are reported in Figs. 7 and 8. The band structure was calculated for several values of the lattice constant a , with c being kept constant at the optimized values of 31.38 a.u. and 95.64 a.u. for hexagonal and cubic phases, respectively. In general, there is no gap at the equilibrium lattice constants ($c/a = 4.02$ and $c/a = 12.26$ for hexagonal and cubic phases, respectively). The energy band gap, however, increases with increasing a (decreasing c/a) up to a maximum value then falls off. For the hexagonal phase, the energy band gap is maximum (~ 0.22 eV) at around $c/a = 3.49$ whereas for the cubic phase, the energy band gap is maximum (~ 0.23 eV) at around $c/a = 10.62$. The dependence of energy band gap on lattice parameters gives an insight into the possibility of tuning the electronic properties of GST for various applications.

The contribution of various orbitals to the band structures of hexagonal and cubic GST systems are also shown in Figs. 4 and 6, respectively, where the *Te 4d* states are considered as semicore. In both phases, the *Ge s*, *Sb s*, *Te s*, *Ge d*, *Sb d* and *Te d* orbitals are located inside the valence band whereas the *Ge p*, *Sb p* and *Te p* orbitals are centered near the Fermi level (~ 7.4 eV). Hence, the *Ge s*, *Sb s*, *Te s*, *Ge d*, *Sb d* and *Te d* electrons are more tightly bound than the *Ge p*, *Sb p* and *Te p* electrons. Specifically, the *Te 5s*, *Sb 4d* and *Ge 3d* orbitals are located deeper in the valence band, suggesting that they are more tightly bound as compared to the *Ge 4s*, *Sb 5s* and *Te 4d* orbitals, which are shifted slightly towards the Fermi level. X-ray photoemission spectroscopy (HX-PES) studies by Kim et al. [34] established that peaks at the lowest binding energy (0 to 6 eV) were due to the *Ge 4p*, *Sb 5p* and *Te 5p* orbitals; peaks at the second

lowest binding energy (6 to 10 eV) are due to the *Ge* 4*s* and *Sb* 5*s* orbitals whereas peaks at the highest binding energy (at 12 eV) are due to the *Te* 5*s* orbital. This is in agreement with this work. Kim et al. [34] confirmed that such a three-peak

structure is characteristic of $(GeTe)_m(Sb_2Te_3)_n$ pseudobinary compounds including $Ge_2Sb_2Te_5$ (GST) which is considered in this study.

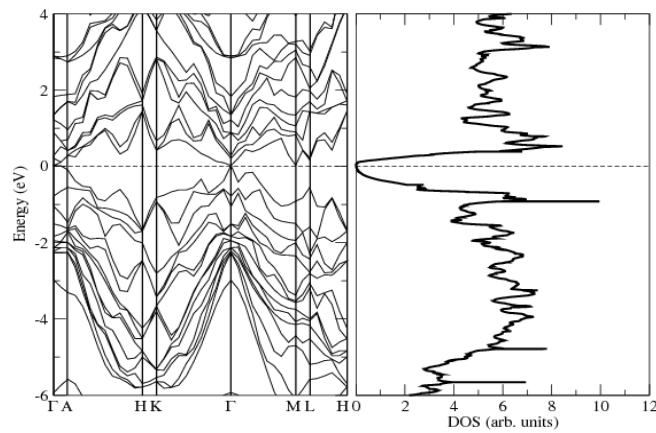


Fig.3: Band structure of hexagonal GST system and the corresponding DOS calculated using LDA for the XC energy functional. The Fermi level is shifted to zero energy.

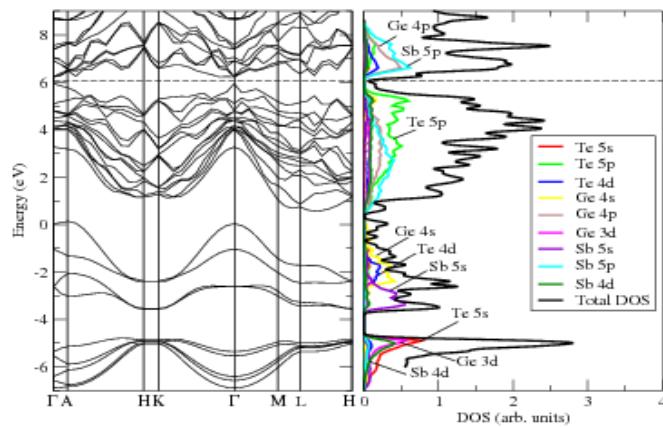


Fig.4: Band structure of hexagonal GST system and the corresponding DOS calculated using GGA for the XC energy functional.

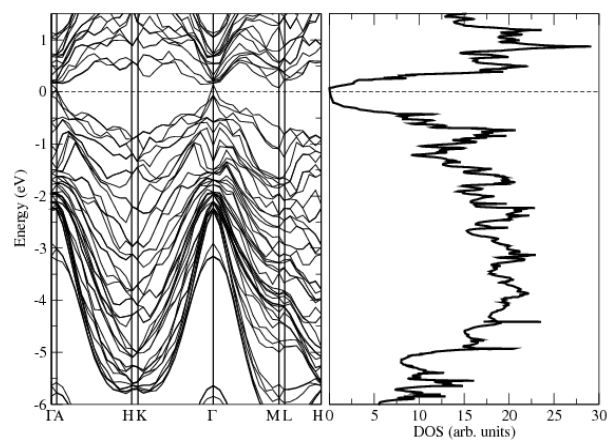


Fig.5: Band structure of cubic GST system and the corresponding DOS calculated using LDA for the XC energy functional. The Fermi level is shifted to zero energy.

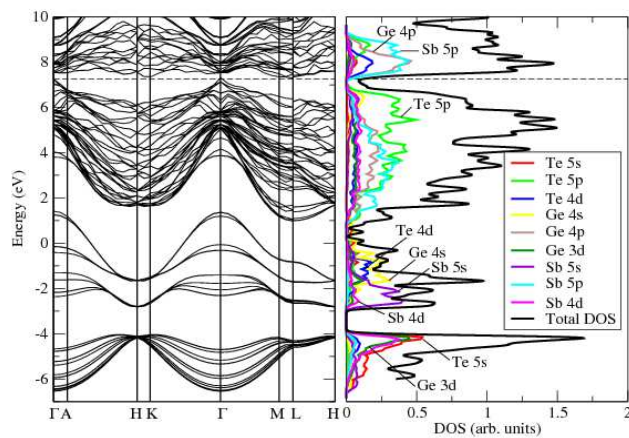


Fig.6: Band structure of cubic GST system and the DOS calculated using GGA for the XC energy functional.

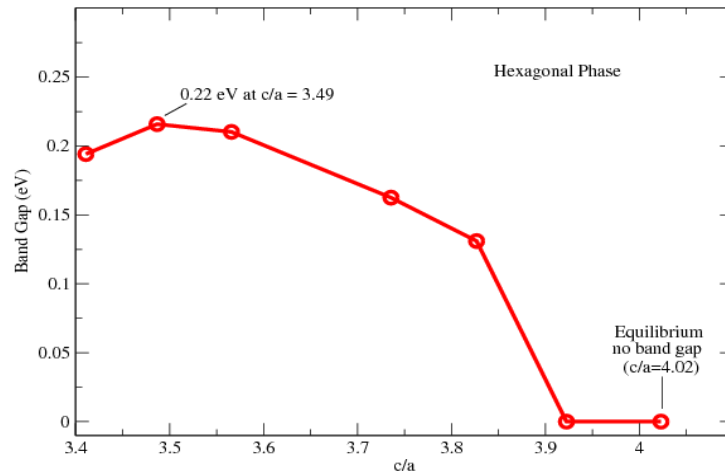


Fig.7: Dependence of energy band gap on lattice parameters c and a for hexagonal GST.

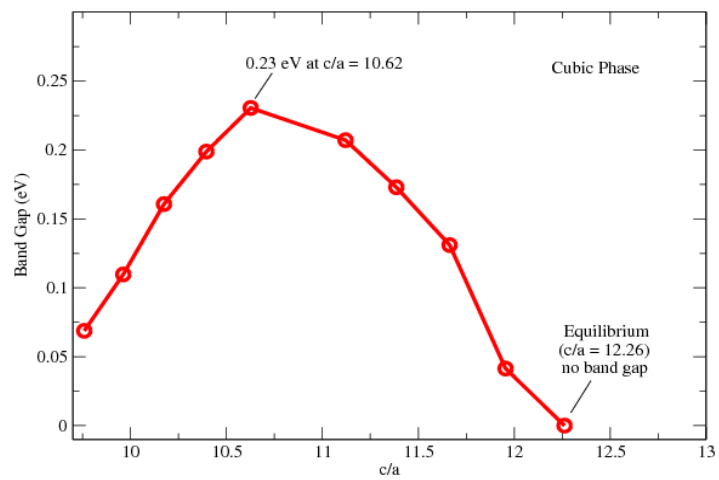


Fig.8: Dependence of energy band gap on lattice parameters c and a for cubic GST.

3.2. Optical properties

The charge density of the unperturbed system was computed at gamma point using a kinetic energy cut-off of 50 Ry for both phases. The calculated absorption spectra for hexagonal and cubic GST are shown in Figs. 9 and 10, respectively. For the hexagonal phase, a major peak at about 0.48 eV and a minor peak at about 1.65 eV are observed using TDDFT whereas the spectrum calculated using GW_0 gave a major peak at about 0.21 eV and a minor peak at about 1.30 eV. For the cubic phase, TDDFT gave a major peak at about 0.66 eV and a minor peak at about 1.70 eV whereas GW_0 gave a major peak at about 0.12 eV and a minor peak at about 1.50 eV. A major absorption peak corresponds to the fundamental absorption edge. Peaks at higher energies in the calculated spectra correspond to optical excitations of unbound states. From our calculated PDOS, $Te s$ orbitals are the most tightly bound as compared to the $Sb s$, $Ge s$, $Te p$, $Sb p$ and $Ge p$ orbitals. Consequently, $Te s$ electrons are, by a large part, not available for bond formation in GST. This is in agreement with the

experimental findings of Sun et al. [14], who established that the valence band of thermally crystallized GST films (cubic phase) is dominated by $Te p$, $Ge p$ and $Sb p$ states with minor contributions from $Ge s$ and $Sb s$ states, whereas the conduction band is mainly populated by anti-bonding $Ge p/Sb p$ states and $Te p$ states. Anti-bonding states are known to be higher in energy and hence less stable than bonding states. Orava et al. [35] have assigned a peak at 1.77 eV in the spectrum of cubic GST system to transitions between $Te p$ bonding states and $Ge p/Sb p$ anti-bonding states. Such a peak is obtained in this study for the cubic GST system at 1.70 eV using TDDFT and at 1.50 eV using GW_0 . Yamanaka et al. [36] have assigned a peak at 1.8 eV in the spectrum of hexagonal GST structure to transitions between $Te p$ and $Sb p$ states. Again, such a peak is obtained in this study for the hexagonal GST system at 1.65 eV using TDDFT and at 1.30 eV using GW_0 .

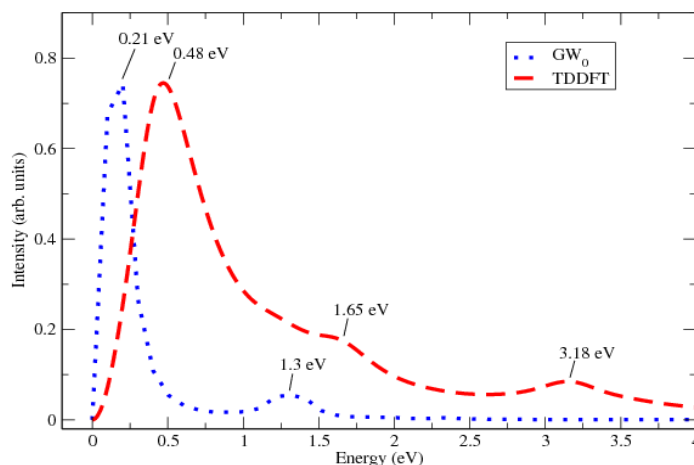


Fig.9: Optical absorption spectra for hexagonal GST calculated using TDDFT and GW_0 .

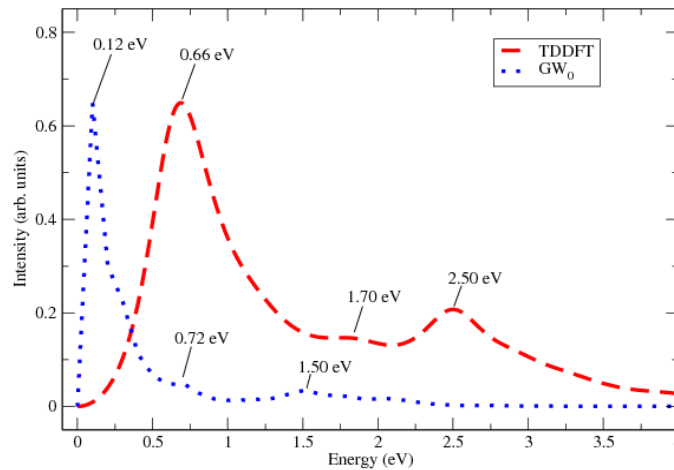


Fig.10: Optical absorption spectra for cubic GST calculated using TDDFT and GW_0 .

4. Conclusions

The electronic band structures of hexagonal and cubic GST systems have been calculated using the LDA and the GGA for the XC energy functional with *Te 4d* electrons treated as core in the former case and as semicore in the latter case. The LDA results give no band gap for both GST phases. However, the GGA results give a band gap of about 0.33 eV at Γ for the hexagonal phase and a band gap of about 0.24 eV at Γ and an indirect band gap of about 0.04 eV along the Γ -K line for the cubic phase. Both LDA and GGA give smaller band gaps as compared to the experimentally determined optical band gap of 0.5 eV for both phases. Using the LDA, it has been shown that the band gap increases to a maximum of 0.22 eV at a *c/a* value of 3.49 for hexagonal GST and 0.23 eV at a *c/a* value of 10.62 for cubic GST. The optical absorption spectra have also been calculated whereby for the hexagonal phase, the absorption edge is found at 0.48 eV using TDDFT whereas it is located at 0.21 eV when GW_0 method is used. For the cubic phase, the absorption edge is located at 0.66 eV and at 0.12 eV using TDDFT and GW_0 , respectively.

Acknowledgements

The authors would like to acknowledge the Center for High performance Computing (CHPC), Cape Town, Republic of South Africa, for compute resources and the developers of QUANTUM ESPRESSO and Yambo codes for the use of the codes.

References

- [1] M. Wuttig and N. Yamada, *Nature Mater.* **6**, 824 (2007).
- [2] S. R. Ovshinsky, *Phys. Rev. Lett.* **21**, 1450 (1968).
- [3] G. I. Meijer, *Science* **319**, 1625 (2008).
- [4] W. Welnic and M. Wuttig, *Materials Today* **11**, 20 (2008).
- [5] A. V. Kolobov, P. Fons, A. I. Frenkel, A. L. Ankudinov, J. Tominaga and T. Uruga, *Nature Mater.* **3**, 703 (2004).
- [6] T. Matsunaga, N. Yamada and Y. Kubota, *Acta Crystallogr. B* **60**, 685 (2004).
- [7] I. I. Petrov, R. M. Imanov and Z. G. Pinsker, *Sov. Phys. Crystallogr.* **13**, 339 (1968).
- [8] B. J. Kooi and T. M. J. de Hosson, *J. Appl. Phys.* **92**, 3584 (2002).
- [9] G. C. Sosso, S. Caravati, C. Gatti, S. Assoni and M. Bernasconi, *J. Phys.: Condens.*

- Matter **20**, 245401 (2009).
- [10] T. Nonaka, G. Ohbayashi, Y. Toriumi, Y. Mori and H. Hashimoto, *Thin Solid Films* **370**, 258 (2000).
- [11] N. Yamada and T. Matsunaga, *J. Appl. Phys.* **88**, 7020 (2000).
- [12] Y. J. Park, Y. J. Lee, M. S. Youm, Y. T. Kim and H. S. Lee, *J. Appl. Phys.* **97**, 093506 (2005).
- [13] A. V. Kolobov, P. Fons, J. Tominaga, A. I. Frenkel, A. L. Ankudinov, S. N. Yannopoulos, K. S. Andrikopoulos and T. Uruga, *Jpn. J. Appl. Phys., Part 1* **44**, 3345 (2005).
- [14] Z. Sun, S. Kyrsta, D. Music, R. Ahuja and J. M. Schneider, *Solid State Comm.* **143**, 240 (2007).
- [15] T. Tsafack, E. Piccinini, B. S. Lee, E. Pop and M. Rudan, *J. Appl. Phys.* **110**, 063716 (2011).
- [16] P. Hohenberg and W. Kohn, *Phys. Rev. B* **136**, 864 (1964).
- [17] W. Kohn and L. J. Sham, *Phys. Rev. B* **140**, 1133 (1965).
- [18] P. Giannozzi, S. Baroni, N. Bonini, M. Calandra, R. Car, C. Cavazzoni, D. Ceresoli, G. L. Chiarotti, M. Cococcioni, I. Dabo, A. Dal Corso, S. Fabris, G. Fratesi, S. de Gironcoli, R. Gebauer, U. Gerstmann, C. Gougoussis, A. Kokalj, M. Lazzeri, L. Martin-Samos, N. Marzari, F. Mauri, R. Mazzarello, S. Paolini, A. Pasquarello, L. Paulatto, C. Sbraccia, S. Scandolo, G. Sclauzero, A. P. Seitsonen, A. Smogunov, P. Umari and R. M. Wentzcovitch, *J. Phys.: Condens. Matter* **21**, 395502 (2009).
- [19] J. P. Perdew and A. Zunger, *Phys. Rev. B* **23**, 5048 (1981).
- [20] J. P. Perdew, K. Burke and M. Ernzerhof, *Phys. Rev. Lett.* **77**, 3865 (1981).
- [21] G. Lee and S. H. Jhi, *Phys. Rev. B* **77**, 153201 (2008).
- [22] G. S. Do, J. Kim, S. H. Jhi, S. G. Louie and M. L. Cohen, *Phys. Rev. B* **82**, 054121 (2010).
- [23] E. van Lenthe, J. G. Snijders and E. J. Baerends, *J. Chem. Phys.* **105**, 6505 (1996).
- [24] H. J. Monkhorst and J. D. Pack, *Phys. Rev. B* **13**, 5188 (1976).
- [25] D. Murnaghan, *Proc. Natl. Acad. Sci. USA* **30**, 224 (1944).
- [26] O. B. Malcioglu, R. Gebauer, D. Rocca and S. Baroni, *Comp. Phys. Comm.* **182**, 1744 (2011).
- [27] A. Marini, C. Hogan, M. Grüning and D. Varsano, *Comp. Phys. Comm.* **180**, 1392 (2009).
- [28] G. D. Lee, M. H. Lee and J. Ihm, *Phys. Rev. B* **52**, 1459(1995).
- [29] R. Khenata, A. Bouhemadou, M. Sahnoun, A. H. Reshak, H. Baltache and M. Rabah, *Comp. Mater. Sci.* **38**, 29 (2006).
- [30] B. S. Lee, J. R. Abelson, S. G. Bishop, D. H. Kang, B. Cheong and K. B. Kim, *J. Appl. Phys.* **97**, 093509 (2005).
- [31] T. Kato and K. Tanaka, *Jpn. J. Appl. Phys.* **44**, 7340 (2005).
- [32] C. Friedrich and A. Schindlmayr, *Many-Body Perturbation Theory: The GW Approximation*, Published in: J. Grotendorst, S. Blügel and D. Marx, *Computational Nanoscience: Do It Yourself, NIC Series* **31**, 335 (2006).
- [33] J. W. Park, S. H. Eom, H. Lee, J. L. F. Da Silva, Y. S. Kang, T. Y. Lee and Y. H. Kang, *Phys. Rev. B* **80**, 115209 (2009).
- [34] J. J. Kim, K. Kobayashi, E. Ikenaga, M. Kobata, S. Ueda, T. Matsunaga, K. Kifune, R. Kojima and N. Yamada, *Phys. Rev. B* **76**, 115124 (2007).
- [35] J. Orava, T. Wagner, J. Sik, J. Prikryl, M. Frumar and L. Benes, *J. Appl. Phys.* **104**, 043523 (2008).
- [36] S. Yamanaka, S. Ogawa, I. Morimoto and Y. Ueshima, *Jpn. J. Appl. Phys.* **37**, 3327 (1998).

Received: 13 August, 2014

Accepted: 10 April, 2015